IOPscience iopscience.iop.org

Home Search Collections Journals About Contact us My IOPscience

MBE grown GaAs on GaAs (001): UHV X-ray diffraction measurements

This article has been downloaded from IOPscience. Please scroll down to see the full text article.

1992 J. Phys.: Condens. Matter 4 4221

(http://iopscience.iop.org/0953-8984/4/17/001)

View the table of contents for this issue, or go to the journal homepage for more

Download details:
IP Address: 171.66.16.96
The article was downloaded on 11/05/2010 at 00:12

Please note that terms and conditions apply.

J. Phys.: Condens. Matter 4 (1992) 4221–4232. Printed in the UK

MBE grown GaAs on GaAs (001): UHV x-ray diffraction measurements

R Bloch, L Brügemann, W Press, M Tolan, K-M Behrens, J Olde and M Skibowski

Institut für Experimentalphysik, Christian-Albrechts-Universität Kiel, Leibnizstrasse 19, D-2300 Kiel 1, Federal Republic of Germany

Received 18 June 1991, in final form 28 November 1991

Abstract. MBE grown gallium arsenide crystals with (001) orientation were investigated with a three-crystal x-ray diffractometer under UHV conditions. In the region of total external reflection ($Q < 0.3$ Å^{-1}) no Kiessig fringes occur and hence no electron density difference between the substrate and the MBE layer exists. In the tails of the 004 Bragg reflection, modulations are observed. They are ascribed to a phase shift at the substrate–layer interface originating from a misfit parallel to the surface normal or a thin intermediate layer. The method can be applied to other thin film systems like oxidized or buried layers.

1. Introduction

The surface quality of gallium arsenide (GaAs) crystals is of great interest both in semiconductor technology and in the physical sciences. Most of the experimental and theoretical work has been performed on the (110) surface of GaAs. This is due to the simplicity of the preparation of smooth and clean (110) surfaces by cleaving the crystals under ultra-high vacuum (UHV) conditions. For electronic devices the (001) plane is more important; this plane is not cleaveable and molecular beam epitaxy (MBE) has to be used for preparation of surfaces of reasonable quality.

In this paper we report investigations on three differently prepared GaAs (001) crystals. The surfaces of the samples initially were characterized by reflection high energy electron diffraction (RHEED) during preparation in UHV. The main concern was to obtain more complete information about the MBE layers by x-ray diffraction. For this purpose, a three-crystal diffractometer (TCD) with the sample under UHV conditions was used. Two different kinds of measurements are performed: total external reflection experiments which are particularly sensitive to differences of the electron density of the MBE layer and the substrate, and Bragg scattering which inherently depends on the crystalline structure of layer and substrate.

2. Samples

For the sample preparation we used mechano-chemically polished GaAs (001) wafers, purchased from Wacker-Chemitronic, Burghausen, Federal Republic of Germany.

0953-8984/92/174221+12$04.50 © 1992 IOP Publishing Ltd

As a first step a wafer was cut into several pieces. The samples were degreased in a subsonic cleaner with trichlorethylene, acetone and methanol; and were then cleaned by de-ionized water. Next, the pieces were mounted on sample holders and transferred into the UHV chamber. Once the bake-out was complete, the sample was further cleaned by sputtering with 1 keV argon ions for several hours. The surface was then ready for MBE. The MBE system had been equipped with evaporation sources for gallium and for arsenic (As_4 and As_2). The base pressure in the UHV chamber was in the range of 10^{-10} mbar except during preparation. The quality of the surface was monitored by RHEED.

Following this standard procedure the three samples were treated differently. These final preparation steps are described in detail below:

(i) Sample A was annealed for 30 min at about 770 K with an As partial pressure of 5×10^{-7} mbar. This treatment yielded a weak 2×4 reconstruction observed by RHEED. This sample served as a reference.

(ii) On Sample B a single crystalline layer was grown by MBE. The growth was performed with an As_4 partial pressure of 5×10^{-7} mbar and a substrate temperature of about 770 K. The growth time for one monolayer was 9–13 s as can be deduced from the RHEED oscillations (see figure 1). The precise value depends on the temperature of the Ga source. This treatment yielded a 2×4 reconstruction, again observed with RHEED [1], which was stable down to room temperature.

(iii) Sample C was also treated by MBE, but an additional thermal cracker was used to break up the As_4 molecules into dimers. With an As_2 partial pressure of 5×10^{-7} mbar and a substrate temperature of about 770 K the growth time for one monolayer was estimated to be 9 s. This treatment resulted in a 2×4 reconstruction, again observed with RHEED.

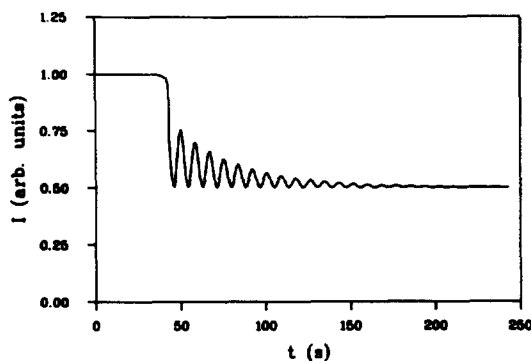

Figure 1. RHEED intensity from GaAs (001) of the specular spot during MBE growth at 8 keV electron energy; As_4 partial pressure 5×10^{-7} mbar, substrate temperature 770 K.

3. Experimental set-up

Figure 2 shows the experimental set-up schematically. The source is a 12 kW x-ray generator with a rotating copper anode. CuKα radiation is extracted by Bragg reflection from a flat Si (111) crystal. Slits of dimensions 10×0.1 mm^2 in front of

and behind the monochromator limit the beam width so that only $CuK\alpha_1$ radiation with the wavelength $\lambda = 1.54056$ Å impinges onto the sample. A flat Si (111) crystal is mounted behind the sample as an analyser and a NaI scintillation counter serves as detector. Lead shields around the monochromator as well as around the detector system and the vacuum beam pipes are installed to reduce the background radiation.

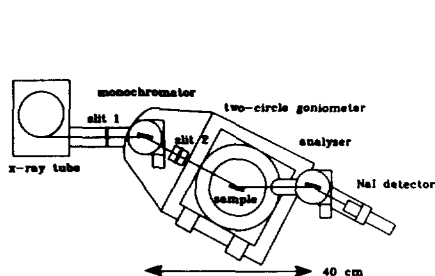

Figure 2. Schematic drawing of the three-crystal diffractometer (top view).

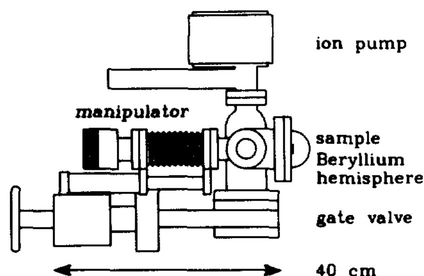

Figure 3. Schematic drawing of the UHV measurement chamber (side view).

The sample was fixed in a small UHV chamber designed in a similar manner to those used at the Hamburger Synchrotronstrahlungslabor (HASYLAB) [2]. The chamber was mounted on a large goniometer head driven by stepping motors. Figure 3 schematically shows the UHV measurement chamber ('baby chamber'). This baby chamber consists of three major components:

(i) A 180° wide Beryllium hemisphere with a diameter of 63 mm which allows the use of several different scattering geometries.

(ii) A sample manipulator for translating the sample from the transfer plane into the centre of the beryllium hemisphere and for rotating the sample around its surface normal.

(iii) A battery-operated ion pump with a pumping rate of $5\ \mathrm{l\ s^{-1}}$.

4. Measurements and discussion

4.1. Total external reflection

In order to determine the electron density profile parallel to the surface normal and the surface roughness of the topmost layer we measured the reflectivity of the samples in the region of total external reflection (critical angle $\theta_c \approx 0.3°$) up to a momentum transfer $Q = 0.3$ Å^{-1}.

The momentum transfer Q is defined by

$$\boldsymbol{Q} = \boldsymbol{k}_f - \boldsymbol{k}_i \qquad \text{with} \quad Q = 4\pi \sin\theta / \lambda.$$

The subscripts i and f denote the initial and final wave vector $\boldsymbol{k}$ of the incident and scattered x-rays ($k_i = k_f = 2\pi/\lambda$). θ is the angle between the incident beam and the surface of the sample and 2θ is the scattering angle.

For the quantitative data analysis we have used a recursive algorithm based on modified Fresnel equations, as developed for layered systems by Parrat [3]. This algorithm is described in detail in [4] and therefore need not be presented here. The parameters of the model were evaluated by use of a least-squares-fit procedure. A χ^2 function

$$\chi^2 = \frac{1}{N}\sum_{i=1}^{N}\delta_i^2 \qquad \text{with} \quad \delta_i = \frac{\log(y_i) - \log(f(x_i, p_1, \ldots, p_M))}{\Delta y_i} \tag{1}$$

was minimized.

In (1) the δ_i are the deviations of the experimental data y_i from the theoretical values $f(x_i, p_1, \ldots, p_M)$ on a logarithmic scale taken at the positions x_i and weighted by the experimental errors Δy_i. Δy_i was estimated to be 5% of y_i. The p_i are the parameters specifying the model. The quantities $\log(y_i)$ were used instead of y_i in order to deal with the large dynamical intensity range of 10^{-7} to 1 in an appropriate way.

The reflected intensity in the region $Q < 0.3$ Å^{-1} is particularly sensitive to the roughness of the topmost surface, and therefore it must be included explicitly in the calculations . Two different descriptions of the surface roughness were combined with the recursive algorithm presented in [4]:

(i) The influence of the surface roughness on the reflected intensity can be taken into account by a static Debye–Waller factor

$$D = \exp\left(-\Delta z^2 Q^2\right) \tag{2}$$

with the mean-square surface roughness parameter Δz. Equation (2) can be obtained if a Gaussian height distribution function around the mean surface plane is assumed. Then Δz describes the average deviation from this mean surface [5–7].

(ii) Another way of describing the surface roughness can be adapted from Wu and Wepp [8]. They introduced a transition layer of thickness t between two media with refractive indices n_1 und n_2. Here the refractive index varies continuously as

$$n(z) = \tfrac{1}{2}(n_2 + n_1) + \tfrac{1}{2}(n_2 - n_1)\tanh\left(-\pi + \frac{2\pi z}{t}\right) \qquad z \in [0, t]. \tag{3}$$

For numerical calculations with the above algorithm the transition region is subdivided into 20 layers with discrete n-values, given by (3). In the present case the interface is the surface–vacuum interface of the sample ($n_2 = 1$, n_1 is the refractive index n of GaAs, see below).

The use of a transition layer model has two main advantages in comparison with a description in terms of a Debye–Waller factor. First, the boundary curvature is not restricted to be much smaller than the wavelength used. Furthermore any other continuous transition function can be tried in (3) [9]. Due to the fact that the meanings of t and Δz (thickness of a transition layer and root mean square roughness) are different, their values are also different. Although each quantity is appropriate to characterize a rough surface it seems to be useful to do the fit procedure with both models, to obtain more reliability in determining the surface roughness.

As an example, figure 4 shows the measured reflectivity of sample C (dots) together with the result of the least-squares fit procedure (solid line), both on a logarithmic scale. The background and the diffuse scattering were subtracted from the measured data. For small Q, a sinusoidal increase of the reflected intensity is observed. This effect is purely geometrical and is related to the part of the incident beam 'seen' by the sample and undergoing total external reflection. This is taken into account by two parameters, the cross-section of the beam and the size of the sample. Beyond the critical angle of total external reflection θ_c ($Q_c = 0.044$ Å^{-1}) the intensity decreases rapidly as predicted by the Fresnel equations.

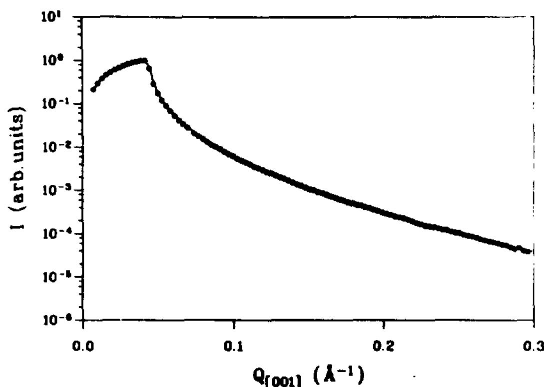

Figure 4. The reflectivity of sample C measured in the region of total external reflection as a function of Q. The solid line is a calculation using the model with a transition layer t. The fit parameters are given in table 1.

A very important result, as will be seen later, is the monotonous decrease of the intensity beyond θ_c. No Kiessig-fringe-like modulations of the reflected intensity are visible [10]. Obviously the density difference $\Delta\rho$ between the MBE grown GaAs layer and the substrate GaAs is small: modulations would be visible, if $\Delta\rho/\rho \geqslant 1\%$. The model calculations, therefore, can be restricted to the reflectivity from a single homogeneous (but rough) surface.

The following model parameters have been utilized: (i) the dispersion term δ of the index of refraction $n = 1 - \delta - i\beta$ and (ii) the roughness parameter Δz or the vacuum–surface transition layer thickness t. The wavelength used, $\lambda = 1.54056$ Å, is far away from the absorption edges of Ga and As. The absorption term β in n is not varied independently because both optical constants δ and β are proportional to the density.

Table 1 shows the results for the three samples. In the fitting procedure reference sample A has been found to be perfectly smooth. The roughness parameter Δz and the thickness t of the transition layer were fitted to values close to zero and the index of refraction is found to be close to the value reported for bulk GaAs ($\delta = 14.52 \times 10^{-6}$, $\beta = 4.19 \times 10^{-7}$) [11]. This smoothness shows that the surface destruction by ion sputtering is removed by the thermal treatment.

On the other hand, the full width at half maximum (FWHM) of the rocking curve (θ scan with 2θ fixed) of sample A of 0.009° is twice as large as the FWHM of the rocking curve of sample C, both measured near θ_c. This suggests imperfection in the surface of the substrate crystals. Possible explanations are either amorphous

Table 1. Results of the fit of the reflectivity measured in the region of total external reflection for the three GaAs crystals. δ and β are the optical constants, Δz and t are the roughness parameters of the different models (static Debye–Waller factor and interface roughness).

Sample	δ ($\times 10^{-6}$)	β ($\times 10^{-7}$)	Δz (Å)	t (Å)
A	14.49±0.02	4.20±0.01	0.31±0.15	—
	14.54±0.02	4.20±0.01	—	2.2±1.0
B	14.57±0.05	4.23±0.02	6.8±0.10	—
	14.49±0.03	4.20±0.01	—	28.6±0.2
C	14.39±0.05	4.17±0.02	2.9±0.10	—
	14.50±0.02	4.20±0.01	—	13.1±0.1

regions or slightly misoriented crystallites in an otherwise single crystalline surface. Such defects may be remnants of the sputtering process and cause a widening of the rocking curve near total external reflection.

The suggestion that the crystal surface shows some residual damage by the ion sputtering despite the following annealing is supported by additional measurements around the reciprocal lattice point 004. An asymmetrical intensity profile parallel to the scattering vector Q was found. Most likely this is due to a concentration of defects in the near surface region of the crystal. Furthermore, perpendicular to Q, some small intensity maxima appeared over a distance of about $1/100°$ from the main maximum. Typically, their intensity is about four orders of magnitude smaller than that of the main maximum. This means that slightly tilted domains exist in an otherwise crystalline structure.

Compared to the RHEED patterns, which indicate a crystalline surface, the x-ray experiment is much more sensitive to deviations from crystallinity.

For the MBE grown samples B and C small but finite roughness parameters are found. The values for Δz (static Debye–Waller factor model) and the thickness t (transition layer model), are twice as large for sample B as those for sample C. From this we can conclude that the MBE layers grown with use of a cracker cell for As_2 are smoother than those produced with a standard As_4 source.

A difference between the ion sputtered sample A and the MBE grown samples B and C can be seen in the rocking curves at the reciprocal lattice point 004. For sample A the x-ray beam was diffracted by a few crystallites which were slightly inclined with respect to one another. The rocking scan from sample C is shown in figure 5. Only the diffraction from a single crystal can be observed. From this we conclude that the MBE grown layer is single crystalline and, also, that there are no misoriented crystallites in the substrate of this sample.

4.2. *Bragg scattering*

Figure 6 shows the Bragg scan of sample B near the reciprocal lattice point 004 on a logarithmic scale. The dots represent the observed intensities, which were again corrected for background and diffuse scattering. The solid line results from the calculation described below. A pronounced modulation of the reflectivity can be seen. As has been already discussed above, we have ruled out a density difference between the MBE layer and the GaAs substrate from the absence of Kiessig fringes in the total external reflection measurements. We, therefore, are led to assume the

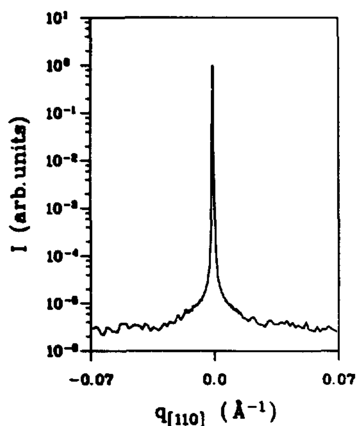

Figure 5. θ scan (rocking curve) at the reciprocal-lattice point 004 for the MBE grown sample C. $q_{[110]}$ is the momentum transfer in [110] direction perpendicular to the surface normal.

existence of a small phase shift between waves reflected by the MBE layer and waves reflected by the substrate. Consequently the scattering is as if there are two crystals slightly displaced with respect to one another perpendicular to their boundary.

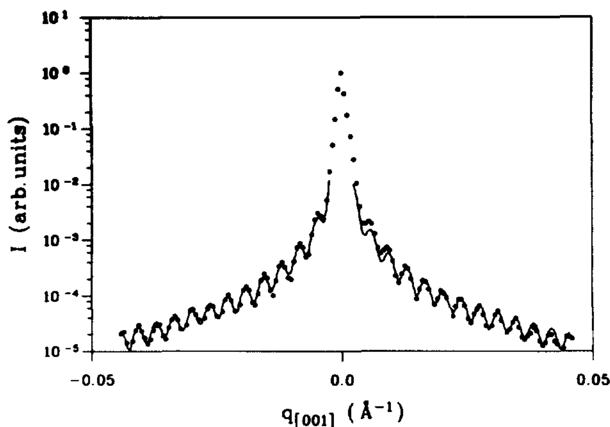

Figure 6. $\theta - 2\theta$ (Bragg) scan of the 004 reflection of sample B. The solid line is the result of the CTR calculation described in the text. The fit results are given in table 2. q is the momentum transfer relative to the reciprocal lattice point (see text).

In principle a mismatch of the lattice parameters of the GaAs substrate and the MBE layer would also cause modulations in the reflectivity near the reciprocal lattice points. But such a lattice mismatch leads to a second Bragg maximum close to the substrate peak [12]. With a resolution of $\Delta Q_{res} = 9 \times 10^{-4}$ Å^{-1} parallel to Q at the 004 reciprocal lattice point [13] a lattice mismatch of about 2×10^{-4} Å can be resolved by the TCD used. Hence, lattice mismatches of this magnitude or above can thus be excluded as the origin of the observed modulations.

A microscopic model for the origin of the phase shift is not available as yet. One may speculate that there are defects, oxides, or deviations from the GaAs stoichiometry. With no detailed model for the transition from the substrate GaAs to the MBE layer we proceed to a rather simplistic calculation which neglects the scattering from

the intermediate region. Then the scattering amplitude is obtained by means of a simple kinematical calculation. It is performed by summing over the Bragg scattering of the MBE layer and the Bragg scattering of the substrate crystal, the two being separated by an 'interface' of thickness d_z. The assumption of a phase shift caused by a small parameter d_z is similar to the description of crystal–crystal interface structures given in [14]. Because of the diffraction geometry used, we have to consider the direction parallel to the surface normal, only. Equation (4) gives the result for the one-dimensional structure factor $F(Q, d_z)$:

$$F(Q,d_z) = \sum_{n=1}^{N_M} \exp\{-\mathrm{i}(n-1)Qa\} + \exp\{-\mathrm{i}Qd_z\} \sum_{n=N_M+1}^{N_M+N_S} \exp\{-\mathrm{i}(n-1)Qa\}. \tag{4}$$

a is the lattice constant of GaAs ($a = 5.65315$ Å) [15], N_M the number of lattice layers in the MBE grown crystal and N_S gives the number of lattice layers of the substrate contributing to the scattering which is determined by the scattering depth [16].

The square of $F(Q, d_z)$ is proportional to the reflected intensity

$$I(Q,d_z) \sim |F(Q,d_z)|^2 = \tfrac{1}{2}\sin^{-2}(Qa/2)\{2 - \cos(\zeta) - \cos(\xi) - \cos(\gamma) + \cos(\zeta+\xi) + \cos(\xi+\gamma) + \cos(\zeta+\xi+\gamma)\} \tag{5}$$

with

$$\zeta = QN_M a \qquad \xi = Qd_z \qquad \gamma = QN_S a.$$

Obviously, $I(Q, d_z)$ has its main maxima for $Qa = 2\pi L$ (L is the Miller index, here $L = 4$ corresponds to the 004 reflection). The above expression gives a description of the Bragg scattering including the so-called crystal truncation rod (CTR) [17], which describes the intensity decrease in the tails of the Bragg peak. In the present case there are three crystal terminations (two of the MBE layer and one of the substrate), all contributing to the scattering. To eliminate rapid oscillations caused by the scattering depth $N_S a$ we have to average all terms in (5) over N_S (assumptions: $N_S \gg N_M$, $Qa \neq 2\pi L$). Introducing the deviation q from the exact Bragg position $q = Q - 2\pi L/a$, (5) can be reformulated:

$$|F(q,d_z)|^2 = \tfrac{1}{2}\sin^{-2}(qa/2)\left\{1 + 4\sin^2(\phi)\sin^2(\psi) - \sin(2\phi)\sin(2\psi)\right\} \tag{6}$$

with

$$\phi = \frac{qN_M a}{2} \qquad \psi = \left(\frac{q}{2} + L\frac{\pi}{a}\right) d_z.$$

The first term in brackets represents the monotonous intensity decrease of the CTR like q^{-2} (q is small in the vicinity of the Bragg peak), which is the standard q-dependence without surface roughness [17]. The further discussion of (6) can be simplified by neglecting terms with qd_z in ψ. This is justified, because both d_z and

q are small. The approximation ($\psi = Ld_z\pi/a$) leads to an easier discussion of (6) and the following reformulation is used:

$$|F(q,d_z)|^2 = \tfrac{1}{2}\sin^{-2}(qa/2)\left\{1 + 2\sin^2(\psi) - 2\sin(\psi)\sin(2\phi + \psi)\right\}. \quad (7)$$

Here the intensity is described by the sum of a q-independent part given by the first two terms in the curly brackets and an oscillating part caused by the thickness $N_M a$ of the MBE layer. From (7) we determine positions q_m of the maximum of these oscillations

$$q_m = \frac{1}{N_M a}\left\{(4m-1)\frac{\pi}{2} - Ld_z\frac{\pi}{a}\right\} = \left(m - \tfrac{1}{4}\right)\Delta q - \delta q$$

$$m = 0, \pm 1, \pm 2, \ldots \quad (8)$$

with the modulation period $\Delta q = q_{m+1} - q_m = 2\pi/N_M a$ and the phase $\delta q = \pi L d_z/N_M a^2$. If $\delta q \neq 0$ the oscillation is remarkably asymmetric with respect to the reciprocal lattice point ($q = 0$) and depends on d_z. This asymmetry allows d_z to be determined by a fit. Unfortunately, the value of d_z can only be determined modulo $\tilde{m}a/L$ ($\tilde{m}$ integer) because $d_z + \tilde{m}a/L$ and d_z lead to the same phase δq in (8). The amplitude A of the modulation also depends on d_z. From (7) we find an amplitude $A = 2\sin(Ld_z\pi/a)$.

In order to compare calculation and experiment directly several extensions of (7) are necessary. One has to include the absorption of the x-rays, a polarization factor, a Lorentz factor and the finite q-resolution of the experimental set-up. Additionally, a static Debye–Waller factor with the parameter Δz accounts for the roughness. Table 2 shows the results for the thicknesses and the roughness parameters.

Table 2. Results of the Bragg fit intensities of the 004 reflection for the MBE grown layers. d is the thickness of the MBE layer and d_z is the displacement between layer and substrate, which gives rise to a phase shift (see text). Here, the roughness was included by using a static Debye–Waller factor with parameter Δz.

Sample	d (Å)	Δz (Å)	d_z (Å)
B	1755±10	9.7±0.7	0.21±0.02
C	1390±10	4.7±0.7	0.43±0.02

From the scattering around the 004 reflection, the thickness of the MBE layer of sample B has been found to be $d = N_M a = 1755 \pm 10$ Å. This is in rather good agreement with the thickness calculated from the RHEED oscillations, which were measured during the MBE growth. For the thickness of the MBE layer of sample C we obtain $d = 1390 \pm 10$ Å from the fit.

For reasons discussed above, d_z must have values between 0 and $a/L \cong 1.4$ Å and can only be determined modulo this value. The agreement of the result for two different samples suggests that the absolute value indeed is very small and may be the same, if the preparation process is the same for different samples.

For both samples, roughness parameters Δz slightly larger than those from total external reflection are obtained. An explanation might be related with the scattering depth near the 004 reciprocal lattice point; this is considerably larger than in the region of total external reflection so that the determined value is an effective roughness, with contributions from the surface and the inner substrate MBE layer interface.

The 004 reflection is sensitive to lattice parameter variations perpendicular to the surface. The (asymmetrical) 113 reflection also has a Q-component parallel to the surface. This allows one to decide whether there is also a deviation between layer and substrate parallel to the surface [18]. Figure 7 shows the measurements of the 113 (dots) and $\bar{1}13$ (solid line) reflections, respectively, for sample C. No significant difference between the measurements is visible.

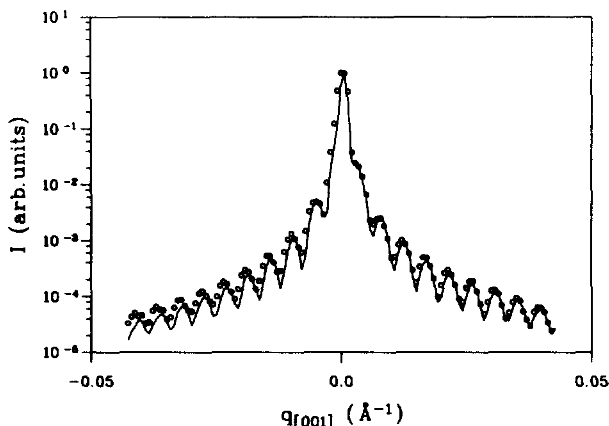

Figure 7. Measurements of the asymmetrical reflections near the reciprocal lattice points 113 (dots) and $\bar{1}13$ (solid line) for sample C. Here $q_{[001]}$ is the momentum transfer in [001] direction, parallel to the surface normal.

The calculation of a CTR at a general Bragg position HKL gives a result virtually identical with that of (5). Only a replacement Qd_z by $\boldsymbol{Q}\boldsymbol{d}$ with $\boldsymbol{d} = (d_x, d_y, d_z)$ and Qa by $\boldsymbol{Q}\boldsymbol{a}$ ($\boldsymbol{a}$ is the vector of the three lattice parameters in x, y, and z direction) in (4) has to be done. As before, the distance between neighbouring intensity maxima yields the modulation period $\Delta q = 2\pi/N_{\mathrm{M}}a$. A fit of the scattering intensity from sample C may serve as an independent determination of the thickness of the MBE layer. Values $d = N_{\mathrm{M}}a = 1435 \pm 12$ Å for the 113 and $d = 1419 \pm 15$ Å for the $\bar{1}13$ reflection are found. They are in satisfactory agreement with the value given in table 2. (Unfortunately no equivalent data are available for sample B.) Figure 7 does not show any significant difference between the modulation around the 113 and $\bar{1}13$ reflection, respectively, especially for the first few modulation periods close to the Bragg peak. Hence we conclude that there is no lateral displacement ($d_x = d_y = 0$). Therefore, d_z can be evaluated modulo $\tilde{m}a/3$ (here $L = 3$) in the case of the 113 reflections. So, combining the results for both types of reflections, d_z can be determined modulo the lattice constant a (d_z modulo $\tilde{m}a/4$ and d_z modulo $\tilde{m}4/3$ yields d_z modulo $\tilde{m}a$). A fit to the 113 reflection gives $d_z = 0.28 \pm 0.03$ Å (statistical errors). This is in rather good agreement with the value given above (table 2).

The following aspects must be taken into account for an assessment of the results of the fits. The given values of the thickness of the MBE layer only depend on the modulation period of the reflection. Due to the great number of visible modulation periods this quantity can be determined rather precisely. The values of d_z depend both on the amplitude A and the phase δq of the modulation. Whereas a quantitative discussion of the phase is rather straightforward, that of the amplitude is more difficult. Two effects, which have not yet been discussed, need to be included. The

first is the resolution of the diffractometer which is $\Delta Q_{res} = 9 \times 10^{-4}$ Å^{-1} near both reciprocal lattice points 113 and 004; this is small in comparison with the modulation period of 4.52×10^{-3} Å^{-1}. The second effect is the reduction of the amplitude of the modulation with increasing q; there are several possible explanations for this, such as waviness of the surface, conformal interface roughness [19] or simply the variations of the MBE layer thickness within the sample area investigated.

As a simple model we have assumed a Gaussian variation of the thickness d of the MBE layer in the fits. Because the values obtained for the roughness (table 2) are about 1% of d, this seems to be justified and is realized mathematically by convoluting the reflection of systems with different MBE layer thicknesses [20]. Such a thickness variation Δd leads to a considerable improvement of the fits and explains the decrease of the amplitude of the modulation with increasing q. The obtained Δd values are of the same magnitude as those of the roughness. All these effects (resolution and thickness variation) lead to a total uncertainty in the d_z determination of about 20%.

Our results show that the crystalline growth of the MBE layer is almost perfect and without distortion or visible strain in all directions. From Bragg scattering, however, we can conclude that the 'inner interface' between substrate and MBE layer is not perfect because this region gives rise to a small phase shift between incoming and outgoing x-rays.

5. Summary and outlook

A three-crystal diffractometer was used to study MBE grown GaAs (001) surfaces.

Measurements in the region of total external reflection were analysed by using Fresnel equations modified for layered systems. With the help of a least-squares fit procedure we could extract the refractive index of the crystals and the roughness parameters of the surface (two models: static Debye–Waller factor and interface roughness). An important result of the total external reflection measurements is that no density difference between MBE layer and substrate is visible.

Bragg scans around reciprocal lattice points different from the origin (here 004, 113, $\bar{1}13$) display a strong modulation, which can be explained by a superposition of waves reflected by the MBE layer and waves reflected by the substrate, and the assumption of a small phase shift between them. This phase shift may be caused by a thin distorted region or a misfit between the MBE layer and the substrate. The thickness $d_z \approx 0.2$ Å of this interface region can be determined modulo $\tilde{m}a$ ($\tilde{m}$ integer) using reflections with different Miller indices. Further information about this region between substrate crystal and MBE layer could be obtained by high resolution electron microscopy.

The sensitivity of the method becomes obvious when oxidizing MBE GaAs surfaces—starting from UHV conditions. A change of the thickness of the crystalline MBE layer (d_z = constant) influences the phase between the modulation and the Bragg peak rather directly. So the method is a sensitive probe of oxidation effects. Similary, the model described in this paper turns out to be a useful approach to the analysis of Bragg scattering from buried layers (see also [15]). A complete report will be published elsewhere.

Acknowledgments

This work was supported by the Bundesministerium für Forschung und Technologie under contract no. 05 401 ABI 2 and by no. 05 401 AAI 1. The authors want to thank D Bahr for helpful discussions.

References

[1] Olde J, Mante G, Barnscheidt H-P, Kipp L, Kuhr J-C, Manzke R, Skibowski M, Henk J and Schattke W 1990 *Phys. Rev.* B **41** 9958
[2] Feidenhans'l R 1986 *PhD Thesis* University of Aarhus, Denmark
[3] Parrat L G 1954 *Phys. Rev.* **95** 359
[4] Bloch R, Brügemann L and Press W 1989 *J. Phys. D: Appl. Phys.* **22** 1136
[5] Beckmann P and Spizzichino A 1963 *The Scattering of Electromagnetic Waves from Rough Surfaces* (London, New York: Pergamon, Macmillan)
[6] Névot L and Croce P 1975 *J. Appl. Crystallogr.* **8** 304
[7] Sinha S K, Sirota E B, Garoff S and Stanley H B 1988 *Phys. Rev.* B **38** 2297
[8] Wu E S and Wepp W W 1973 *Phys. Rev.* A **8** 2065
[9] Andreev A V, Michette A G and Renwick A 1988 *J. Mod. Opt.* **35** 1667
[10] Rieutord F, Benattar J J, Bosio L, Robin P, Blot C and de Kouchkovsky R 1987 *J. Physique* **48** 679
[11] *International Tables for X-Ray Crystallography* 1974 (Birmingham: Kynoch)
[12] Vandenberg J M, Hamm R A, Panish M B and Temkin H 1987 *J. Appl. Phys* **62** 1278
[13] Brügemann L 1989 *PhD Thesis* University of Kiel, Federal Republic of Germany
[14] Weast R C (ed) 1986 *Handbook of Chemistry and Physics* 66th edn (Boca Raton, FL: Chemical Rubber Company)
[15] Robinson I K, Tung R T and Feidenhans'l R 1988 *Phys. Rev.* B **38** 3632
[16] Bartels W J, Hornstra J and Lobeek D J W 1986 *Acta. Crystallogr.* A **42** 539
[17] Robinson I K 1986 *Phys. Rev.* B **33** 3830
[18] Hansson P O, Werner J H, Tapfer L, Tilly L P and Bauser E 1990 *J. Appl. Phys.* **68** 2158
[19] Sinha S K, Sanyal M K, Gibaud A, Satija S K, Majkrzak C F and Homma H unpublished
[20] Tolan M, König G, Brügemann L, Press W, Brinkop F and Kotthaus J P unpublished